



# Investigation of Crack Effects on Isotropic Cantilever Beam

Ehab Samir Mohamed Mohamed Soliman

Submitted: 4 March 2019 / in revised form: 20 July 2019 / Published online: 1 December 2019  
© ASM International 2019

**Abstract** The effect of an open edge crack on the parameters of an isotropic aluminum cantilever beam was investigated. The rotational stiffness and flexibility of the cantilever beam crack were analytically calculated for various crack depths. The results showed that as the depth of the crack increased, the rotational stiffness decreased and flexibility increased. For the intact cantilever beam, acceptable variation was validated by comparing the analytically estimated natural frequencies of the first three modes of bending vibration, and those obtained through modal analysis using the block Lanczos method of finite element analysis software ANSYS v16. The software was used to perform a structural, modal and harmonic analysis of the cracked cantilever beam under different scenarios. The results showed a reduction in the natural frequencies with the existence of the crack. The amount of the reduction varied based on the location and depth of the crack and the pattern of mode shapes. The calculated value of stiffness of the cantilever beam decreased with the presence of the crack. The amount of the decrease was dependent on the depth and location of the crack. The calculated values of the (SIF) stress intensity factor in mode I of the crack (opening edge crack) were proportional to the depth of the crack and inversely proportional to the distance of the crack from the fixed end of the cantilever beam. Based on these results, it is inferred that changes in the modal and structural parameters of the cracked cantilever beam were evidence which could be used to identify cracks.

**Keywords** Rotational stiffness · Modal analysis · Harmonic analysis · Cracked cantilever beam · FEA

## Introduction

Cracks initiated by fatigue are a major problem in the dynamic structure of industrial machinery where they can cause accidents and failures [1]. The vibration behavior of beams changes when cracks occur, so action can be taken to prevent more damage [2]. Natural frequencies and mode shapes can be used to distinguish between healthy and unhealthy structures [3]. Cantilever beams are used in many mechanical structures, and researchers have studied cracked cantilever beams [4–6]. Choudhury et al. [3] carried out a theoretical analysis of a cracked cantilever beam and observed that frequency values change along with crack depth and crack location. They observed changes in frequency behavior in the first three modes of vibrations. Their results indicated that the range of natural frequency increased for different crack locations and depths at higher modes of vibration. They outlined a new optimization method for estimation of results based on location and depth of crack. The maximum error in this proposed method is 0.3 and 0.05% based on crack depth and crack location, respectively. Liu et al. [7] investigated the vibration of a cantilever beam with a closed, fully embedded horizontal crack and developed a new three-segment beam model with local flexibilities at the crack tips. They obtained the natural frequencies and mode shapes of the cracked cantilever beam using the transfer matrix method and compatibility conditions at the crack tips. They determined compliance at the crack tips using a  $J$ -integral approach. They validated the  $J$ -integral approach by comparing their results with those calculated using finite

---

E. S. M. M. Soliman (✉)  
Mechatronics and Robotics Department, Faculty of Engineering,  
Egyptian Russian University, Badr City, Cairo 11829, Egypt  
e-mail: swgezumo@yahoo.com

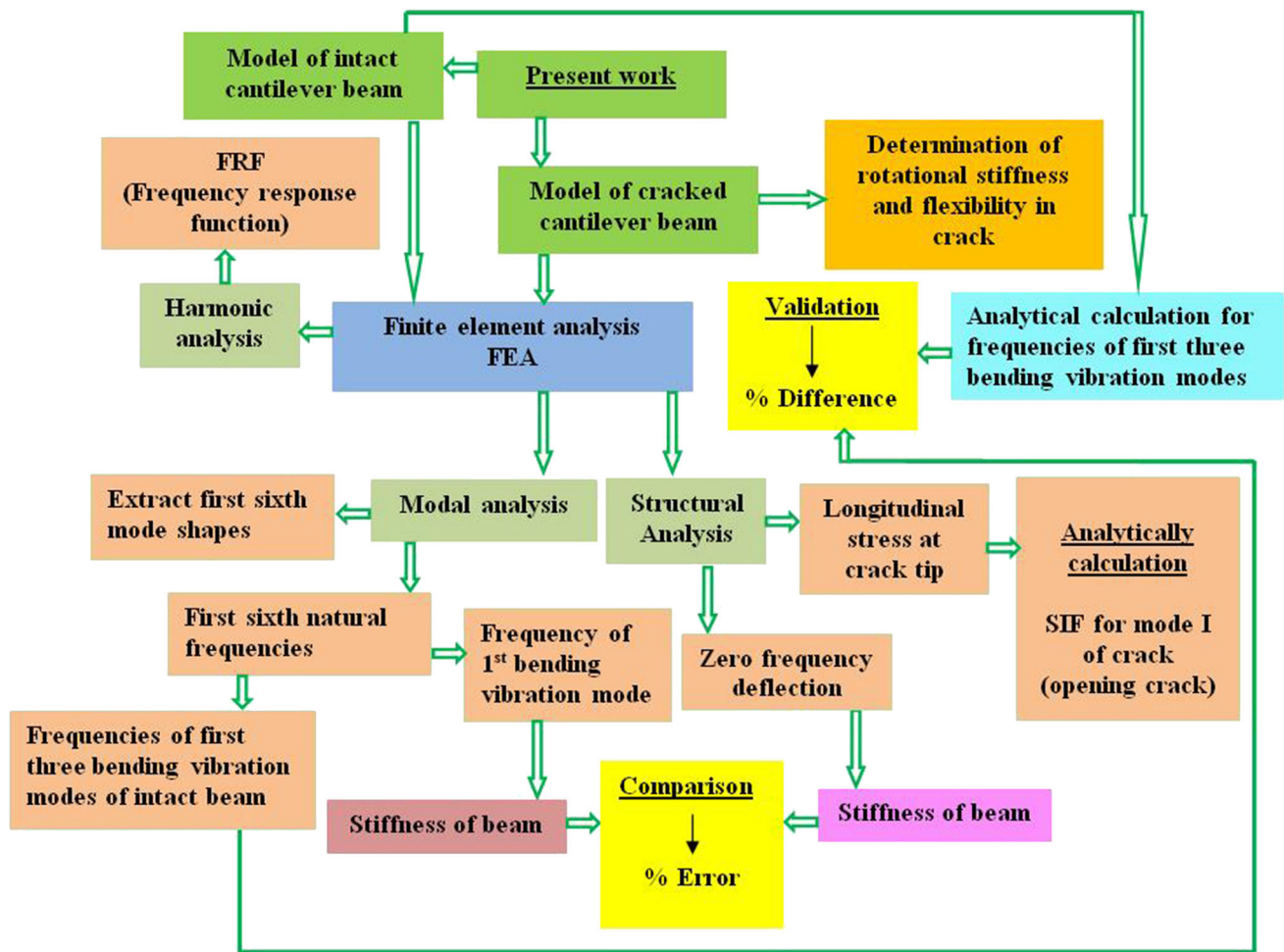
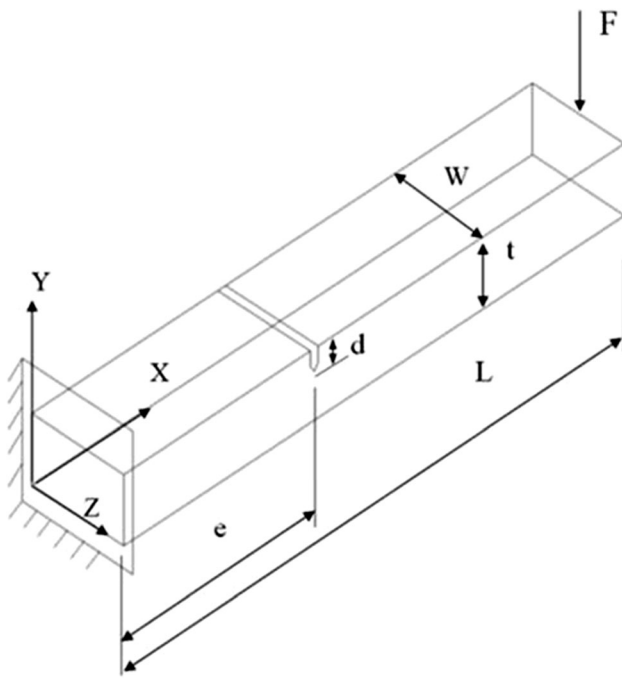


Fig. 1 Schematic of present work

element analysis and found only small differences between the two methods. Zeng et al. [8] established the finite element model of cracked cantilever beams and introduced the use of the area damage factor when evaluating crack levels. They discussed vibration response and crack level identification in three cases of crack severity. They inferred that a combination of the acceleration–velocity phase portraits in the excitation direction and lateral velocity–displacement phase portraits perpendicular to the excitation direction can be used to identify the crack severity. Mia et al. [9] have extracted modal analysis, natural frequencies and mode shapes of transverse vibrations for the first three modes of both intact and cracked cantilever beams. They used commercial finite element analysis software ABAQUS to analyze various crack depths and locations and concluded that natural frequency is reduced when a crack is present. The amount of the reduction depends on the crack location, depth and opening size. Nandwana and Maiti [10] used a rotational spring for modeling transverse vibrations of a slender beam in the presence of an inclined edge or internal normal crack to detect crack location based on

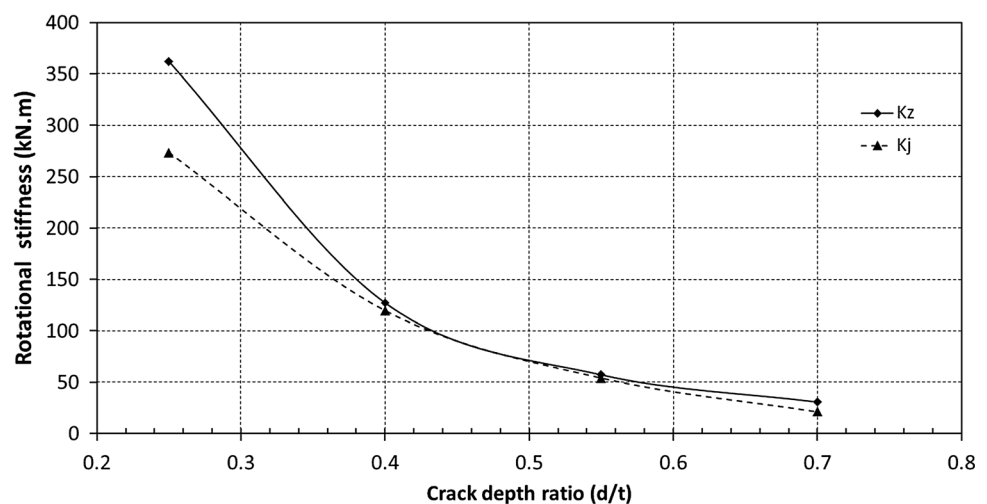
measurement of natural frequencies. They plotted spring stiffness versus crack locations for the three lowest transverse modes. Their prediction of crack location was less than 4.5% when an inclined edge crack was present. Khalkar and Ramachandran [11] investigated the effects of transverse cracks and oblique cracks at different locations and depths on the dynamic responses of the cantilever beam. They observed that when crack depth increases to 80% of the depth of the beam, a significant reduction in the natural frequency of the beam occurs. They also observed that when crack depth is 20% or less of the depth of the beam, the reduction in the natural frequency of the beam is least affected. Batabyal et al. [12] carried out parametric studies using ANSYS software to evaluate natural frequencies and mode shapes for different crack parameters. They plotted the contour lines of the cracked beam frequencies so that any point represents the frequency at a specific crack location and depth. They inferred that both crack location and crack depth have noticeable effects on the modal parameters of the cracked cantilever beam. Djidrov et al. [13] introduced a single transversal crack at



**Fig. 2** Model of cracked cantilever beam

the surface of a cantilever beam and presented changes in natural frequency and FRF amplitude attributable to the effect of different crack depths at different crack positions. Their results indicated that when a crack is located near the middle of the beam, there are noticeable shifts in both FRF amplitude and frequency where the severity of the crack depth is perceptible. In this study, rotational stiffness and flexibility in a crack are analytically calculated and plotted for various crack depth ratios, using a described model on a cracked isotropic aluminum cantilever beam. ANSYS v16 was used to perform finite element analysis (FEA), including calculations of the modal, harmonic and structural frequencies for both the intact and cracked cantilever beams. The natural frequencies for the first three bending

**Fig. 3** Relation between rotational stiffness in crack and crack depth ratio



vibration modes for the intact cantilever beam obtained using FEA were validated with the results obtained through analytical calculations. Modal analysis was used to derive the first sixth mode shapes and its natural frequencies, including the modes of bending vibration, torsional vibration and deformation in Z. The relationship between the frequency ratios and the crack depth ratios was plotted and studied for various crack locations on the cracked beam. Structural analysis was used to calculate zero frequency deflection for the intact and cracked beams. The stiffness of the intact and cracked beams was analytically calculated using zero frequency deflection and the natural frequency of the first mode of bending vibration to determine the percent of error. Deformation response in the Y-direction was plotted and studied for both the intact and cracked beams. Structural analysis was also used to determine longitudinal stress at the crack tips in the cracked cantilever beam. The stress intensity factor for mode I of the crack (opening edge crack) was analytically estimated for the cracked cantilever beam. The schematic for the present work is shown in Fig. 1.

### Description of Model

For this study, the selected isotropic material for the intact and cracked cantilever beams is aluminum. The properties [14] for this material are Young's modulus of elasticity ( $E$ ) = 70 GPa, Poisson's ratio ( $\nu$ ) = 0.346 and density ( $\rho$ ) = 2710 kg/m<sup>3</sup>. The model used for the cracked cantilever beam is shown in Fig. 2. The dimensions and parameters of the intact and cracked cantilever beam are length ( $L$ ) = 600 mm, width ( $W$ ) = 45 mm, thickness ( $t$ ) = 30 mm and load ( $F$ ) = 150 N. In the analytical calculations and finite element analysis, the crack is single transversal, assumed to be open edge, and listed based on

**Fig. 4** Relation between flexibility in crack and crack depth ratio

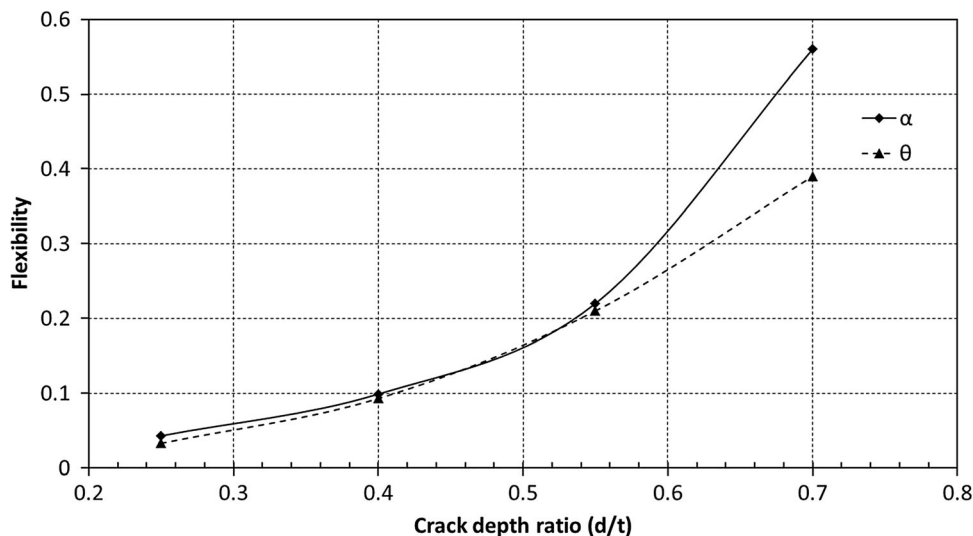
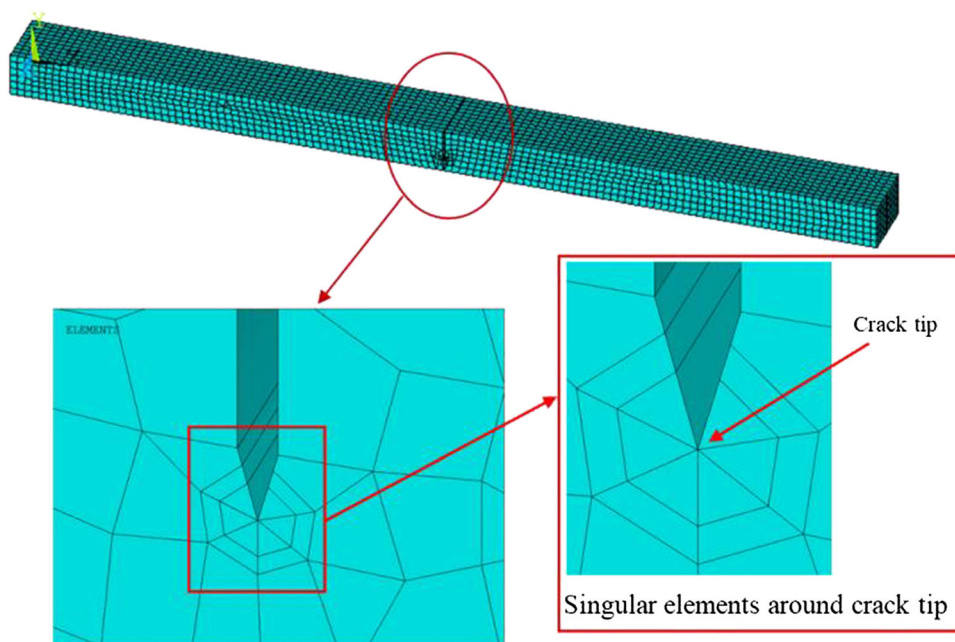


**Fig. 5** FEM model of the cracked beam: (d/t) = 0.7, (e/L) = 0.5



crack depth ratio ( $d/t$ ) and crack location ratio ( $e/L$ ) where  $d$  is the depth of the crack and  $e$  is the distance from the crack to the fixed end of the cantilever beam. For this analysis, the crack is present at crack location ratios of 0.1, 0.5 and 0.9. For every crack location, the crack depth ratio was varied as 0.25, 0.4, 0.55 and 0.7.

**Rotational Stiffness and Flexibility**

Beam cracks can be modeled as equivalent internal springs, and the linear-moment law can be applied when a crack opens [15]. To simulate a uniform depth one-dimensional beam crack, the torsional spring separates an intact beam

**Table 1** Material properties and geometry for cracked cantilever beam model [9]

Property	Value
Length	3 m
Width	0.25 m
Depth	0.2 m
Material	Mild steel
Elastic modulus	$210 \times 10^9$ N/m <sup>2</sup>
Density	7860 kg/m <sup>3</sup>
Poisson’s ratio	0.3

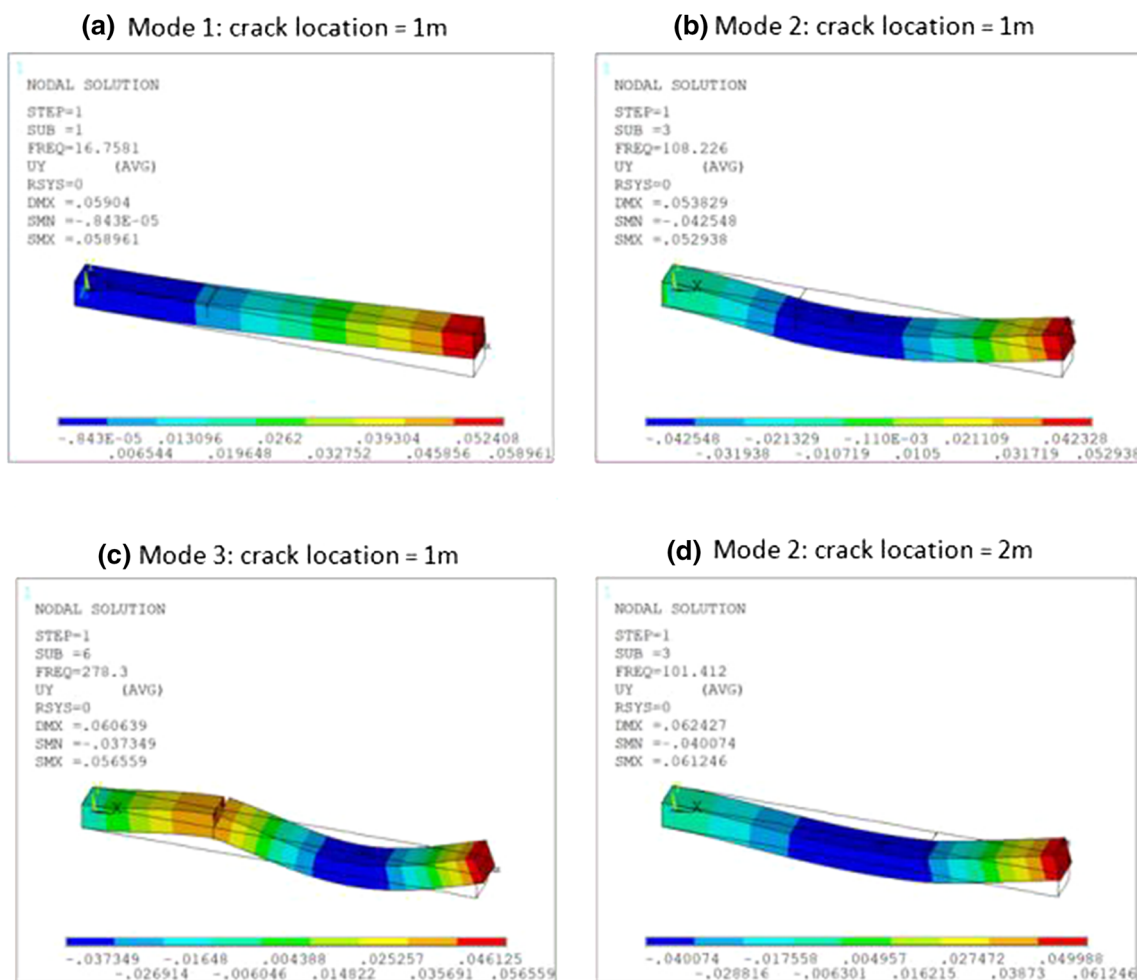


Fig. 6 FEA results for the cracked beam model modes of bending vibration

Table 2 Frequency at different crack locations for crack depth 0.1 m

Crack location from fixed end (m)		Frequency (cycle/s)		
		Mode 1	Mode 2	Mode 3
0.5	Results, [9]	15.686	112.980	305.750
	FEA	15.3948	112.793	305.162
	Variation (%)	1.86	0.17	0.19
1	Results, [9]	16.936	108.77	280.81
	FEA	16.7581	108.226	278.3
	Variation (%)	1.05	0.5	0.89
1.5	Results, [9]	17.917	99.513	310.080
	FEA	17.8092	98.1251	310.093
	Variation (%)	0.6	1.39	-0.0042
2	Results, [9]	18.437	102.65	274.09
	FEA	18.3974	101.412	271.297
	Variation (%)	0.21	1.2	1.02
2.5	Results, [9]	18.6	112.28	285.66
	FEA	18.5791	111.982	283.024
	Variation (%)	0.11	0.27	0.92

into two segments [16]. The approach that replaces the crack with a rotational spring has been used to analyze a cracked beam with a rectangular cross section [17, 18]. In the massless rotational spring model, the stiffness is inversely proportional to the crack size [10]. The presence of the crack in the component is informed by local flexibility [19]. The presence of the crack influences the dynamic response of the system under an external force with constant amplitude and frequency, and local flexibility can then be determined based on crack depth [20]. Flexibility was treated as a dimensionless parameter related to the severity of damage [15]. In this study, rotational stiffness and flexibility in crack were calculated using multiple methods: rotational stiffness using Eq 1 [21] and Eq 2 [15], and flexibility using Eq 3 [21] and Eq 4 [15]. The calculated values of rotational stiffness and flexibility are plotted versus the crack depth ratios in Figs. 3 and 4, respectively, showing that as crack depth increases, rotational stiffness decreases and flexibility increases.

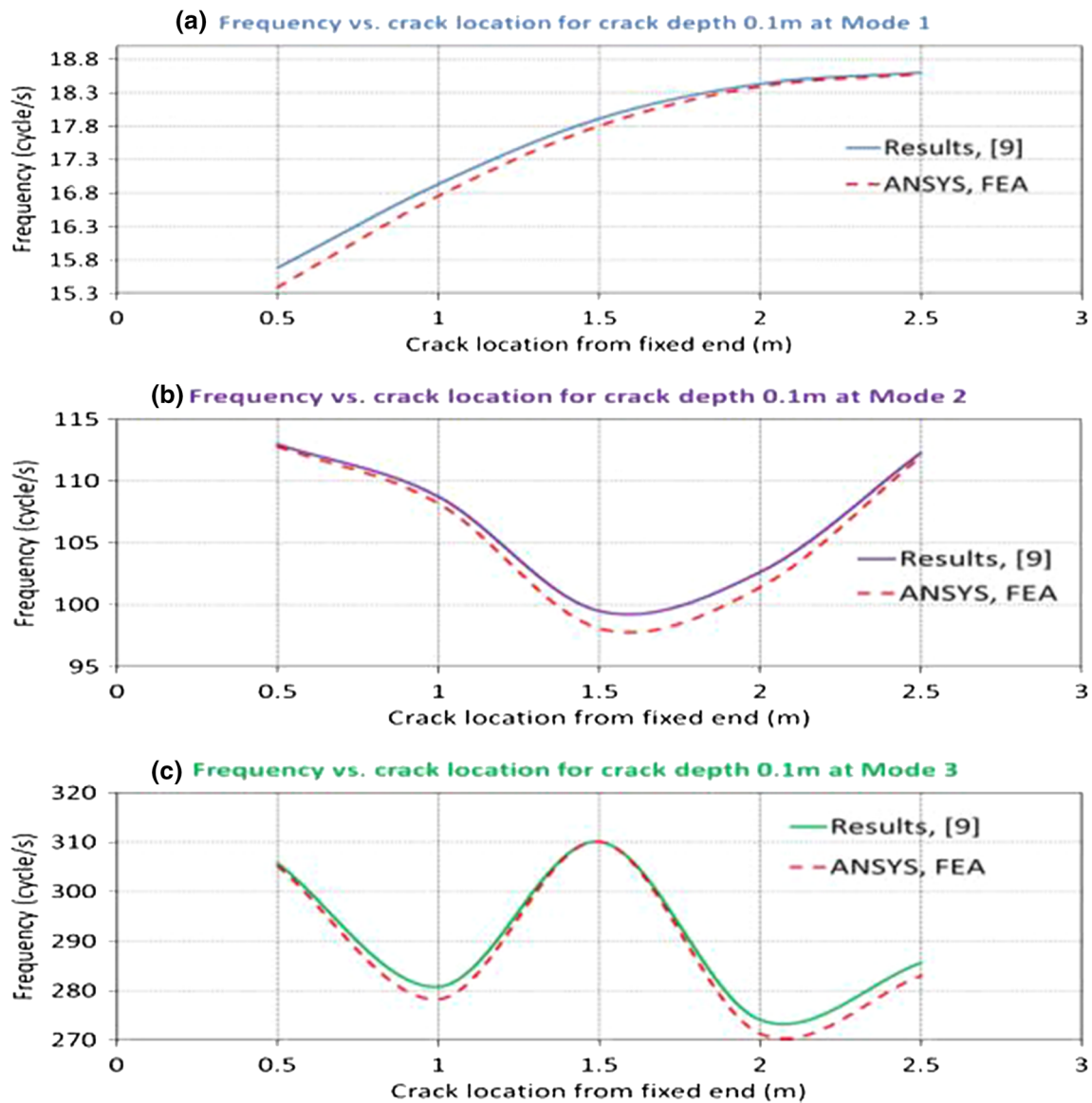


Fig. 7 Frequency vs. crack location for crack depth 0.1 m at the first three modes

Table 3 Comparison between the FEA and analytically natural frequencies of the intact cantilever beam

Natural frequency	Finite element analysis (Hz)	Analytical solution (Hz)	Difference (%)
Natural frequency of first mode of bending vibration	2.1729	2.1644	0.39
Natural frequency of second mode of bending vibration	13.461	13.565	- 0.77
Natural frequency of third mode of bending vibration	37.034	37.938	- 2.4

$$K_z = Wt^2E/72\pi \left(\frac{d}{t}\right)^2 f_z \left(\frac{d}{t}\right) \tag{Eq 1}$$

$$f_z \left(\frac{d}{t}\right) = 0.6384 - 1.035 \left(\frac{d}{t}\right) + 3.7201 \left(\frac{d}{t}\right)^2 - 5.1773 \left(\frac{d}{t}\right)^3 + 7.553 \left(\frac{d}{t}\right)^4 - 7.332 \left(\frac{d}{t}\right)^5 + 2.4909 \left(\frac{d}{t}\right)^6$$

where  $K_z$  is rotational stiffness in crack

$$K_j = \frac{EI}{t} \frac{0.9[(d/t) - 1]^2}{(d/t)[2 - (d/t)]} \tag{Eq 2}$$

$$I = \frac{1}{12} Wt^3, \text{ where } K_j \text{ is rotational stiffness in crack}$$

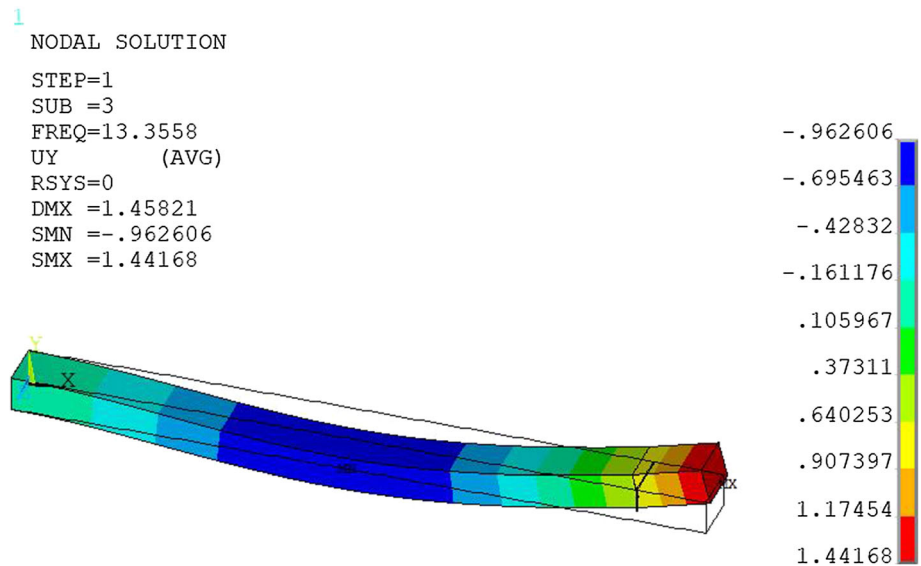
**Table 4** The first sixth natural frequencies for intact and cracked cantilever beam

Object	Natural frequency (Hz)					
	Mode 1 Bending vibration	Mode 2 Deformation in Z	Mode 3 Bending vibration	Mode 4 Deformation in Z	Mode 5 Torsional vibration	Mode 6 Bending vibration
Intact beam	2.1729	3.2455	13.461	19.823	35.111	37.034
Cracked beam: $(d/t) = 0.25, (e/L) = 0.1$	2.0956	3.2003	13.3	19.723	34.839	36.987
Cracked beam: $(d/t) = 0.4, (e/L) = 0.1$	1.9551	3.1294	13.022	19.566	34.411	36.829
Cracked beam: $(d/t) = 0.55, (e/L) = 0.1$	1.7263	3.0233	12.636	19.335	33.753	36.588
Cracked beam: $(d/t) = 0.7, (e/L) = 0.1$	1.3611	2.8647	12.163	19.006	32.793	36.228
Cracked beam: $(d/t) = 0.25, (e/L) = 0.5$	2.1635	3.2394	13.151	19.651	34.984	37.122
Cracked beam: $(d/t) = 0.4, (e/L) = 0.5$	2.1365	3.2274	12.545	19.363	34.757	37.090
Cracked beam: $(d/t) = 0.55, (e/L) = 0.5$	2.08	3.2084	11.508	18.928	34.393	37.050
Cracked beam: $(d/t) = 0.7, (e/L) = 0.5$	1.9432	3.176	9.849	18.263	33.837	37.007
Cracked beam: $(d/t) = 0.25, (e/L) = 0.9$	2.1772	3.2482	13.482	19.829	35.107	37.007
Cracked beam: $(d/t) = 0.4, (e/L) = 0.9$	2.1779	3.2494	13.471	19.825	35.102	36.786
Cracked beam: $(d/t) = 0.55, (e/L) = 0.9$	2.1780	3.2505	13.428	19.813	35.082	36.223

Object	Natural frequency (Hz)					
	Mode 1 Bending vibration	Mode 2 Deformation in Z	Mode 3 Bending vibration	Mode 4 Deformation in Z	Mode 5 Bending vibration	Mode 6 Torsional vibration
Cracked beam: $(d/t) = 0.7, (e/L) = 0.9$	2.1786	3.2516	13.356	19.794	34.566	35.061

**Fig. 8** Third mode shape (second mode of bending vibration): cracked beam;  $(d/t) = 0.7, (e/L) = 0.9$



$$\theta = 6\pi \left(\frac{d}{t}\right)^2 f_z \left(\frac{d}{t}\right) (t/L) \tag{Eq 3}$$

where  $\theta$  is flexibility at crack location

$$\alpha = \frac{EI}{(K_j)L} \tag{Eq 4}$$

where  $\alpha$  is a dimensionless parameter related to the severity of the damage,  $E$  is the modulus of elasticity,  $I$  is the moment of inertia,  $W$  is beam width,  $t$  is beam thickness,  $d$  is crack depth, and  $L$  is beam length.

**Fig. 9** Third mode shape (second mode of bending vibration): cracked beam; ( $d/t = 0.7$ ,  $(e/L) = 0.5$ )

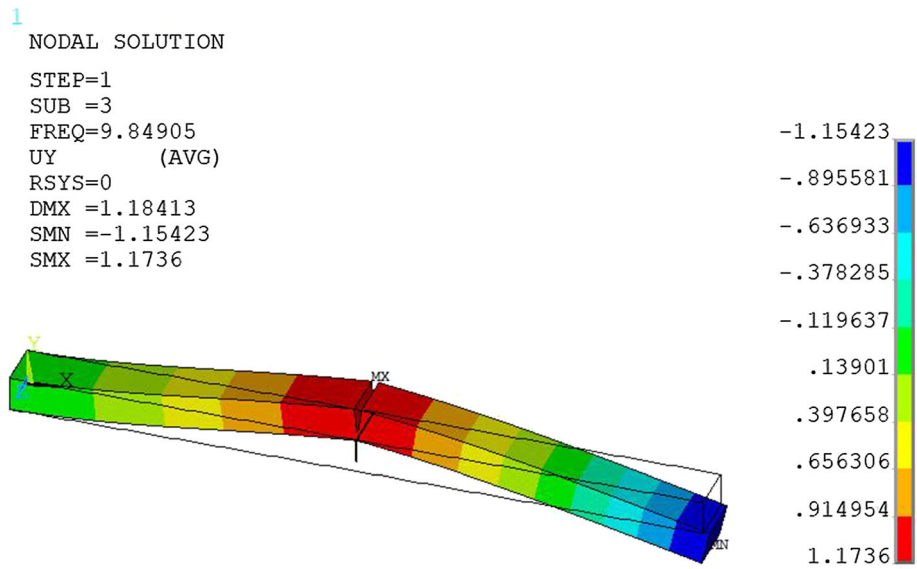
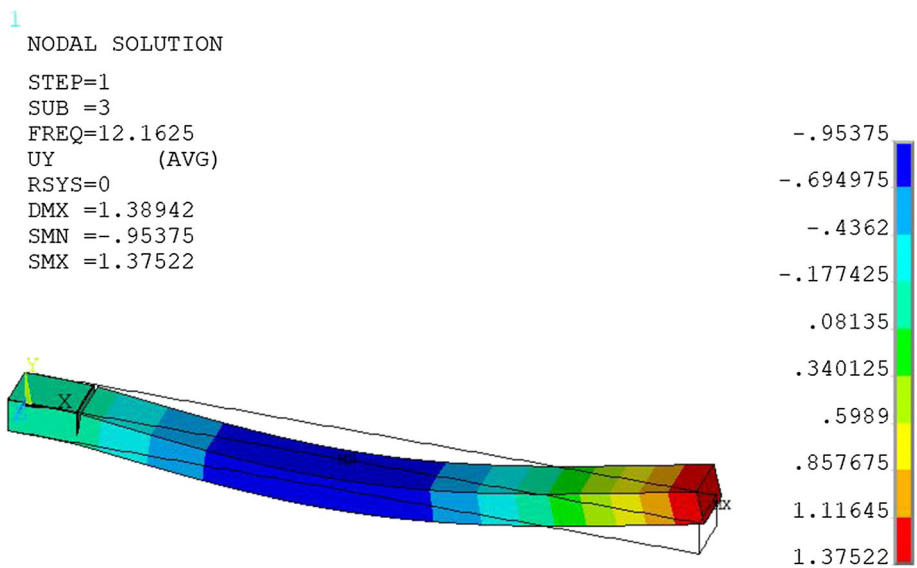


**Fig. 10** Third mode shape (second mode of bending vibration): cracked beam; ( $d/t = 0.7$ ,  $(e/L) = 0.1$ )



**Finite Element Analysis (FEA)**

ANSYS v16 [22] is used to perform finite element analysis (structural, modal and harmonic) of a 3D model of the intact and cracked cantilever beams. The finite element analysis of the cracked cantilever beam is performed at different crack locations and depths. The solid 185 element used in the analysis is suitable for modeling the 3D solid structure and has special features such as large deflection, large strain, plasticity, hyper-elasticity, stress stiffening and fracture parameter calculations. The solid 185 element is defined along eight nodes with three degrees of freedom at each node: translations in the nodal  $x$ ,  $y$  and  $z$  directions.

The region around the crack tip is crucially important in the finite element modeling where it has high gradients of stress and deformation fields. A refined mesh in the region around the crack tip should be used to pick up the rapidly varying stress and deformation fields. In linear elastic problems, the displacements near the crack tip (or crack front) vary as a function of  $\sqrt{r}$ , where  $r$  is the distance from the crack tip. The stresses and strains are singular at the crack tip, varying as a function of  $1/\sqrt{r}$ . The crack faces should be coincident, and the elements around the crack tip (or crack front) called singular elements should be quadratic, with the mid-side nodes placed at the quarter points to capture the singularity in stresses and strains. In the



**Fig. 11** Sixth mode shape (third mode of bending vibration): cracked beam; ( $d/t = 0.55$ ,  $(e/L) = 0.9$ )

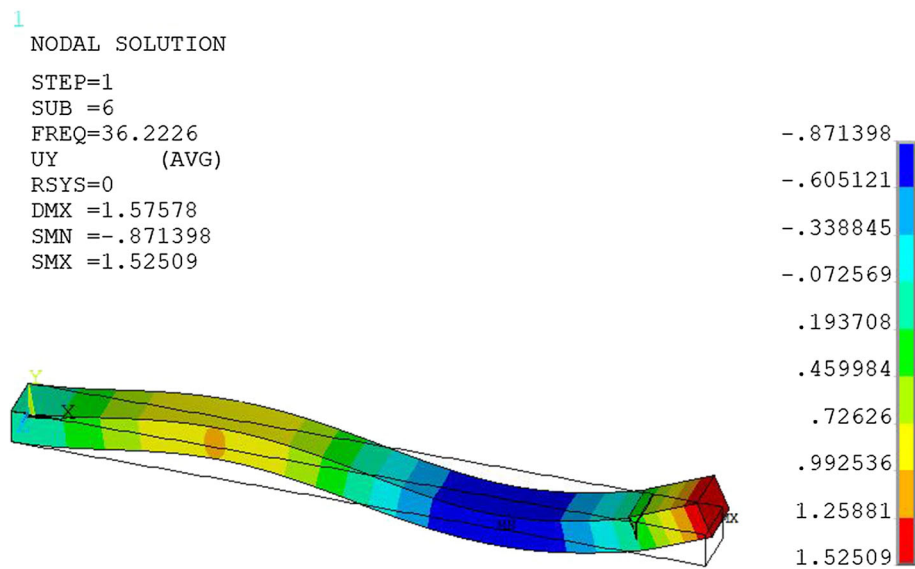
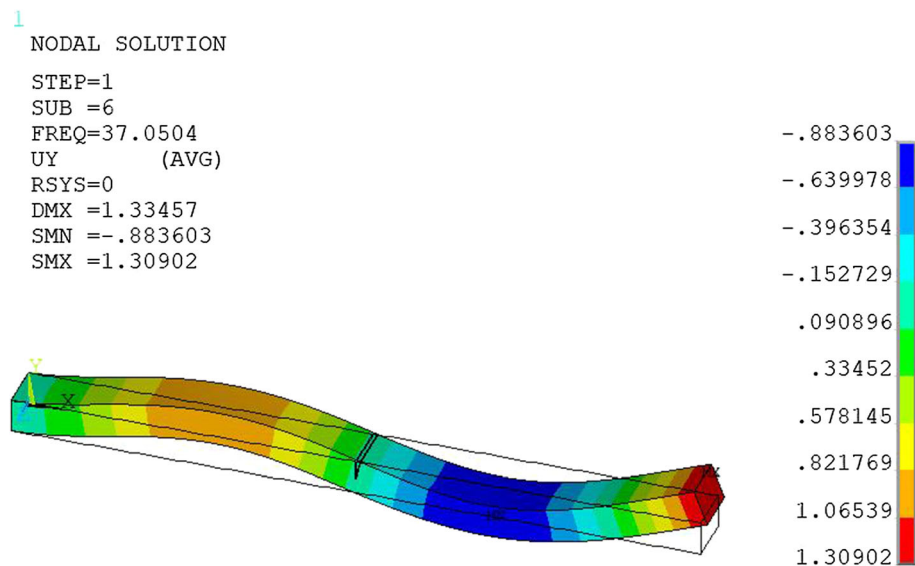


**Fig. 12** Sixth mode shape (third mode of bending vibration): cracked beam; ( $d/t = 0.55$ ,  $(e/L) = 0.5$ )

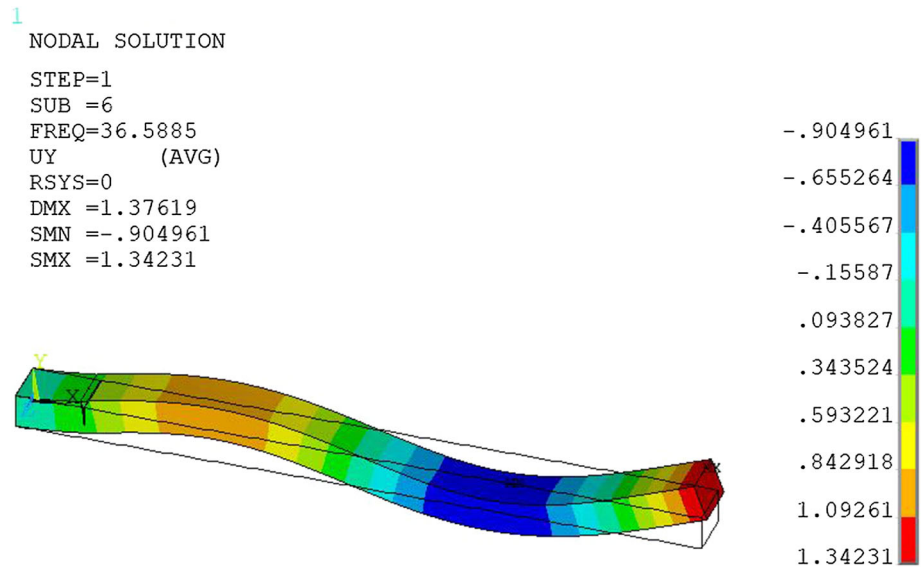


finite element analysis, the singular elements are used for meshing the region around the crack tip, as shown in Fig. 5. For meshing 2D cracked beam model, plane 183 element type is used and then the 2D model is extruded in Z-direction to obtain 3D cracked beam model. The plane 183 element is changed to solid 185 element type for meshing 3D cracked model. The applied load ( $F$ ) = 150 N is applied at the free end of the 3D model of the intact and cracked cantilever beams during structural and harmonic analysis. The cracked beam and its crack tip are meshed in ANSYS v16, as shown in Fig. 5.

### Validation of FEA Results

A comparison between the ANSYS FEA natural frequencies of the first three modes of bending vibration and those obtained by Mia et al. [9] for cracked cantilever beam model is carried out. The material properties and geometry for the cracked cantilever beam model are given in Table 1 [9]. In the finite element analysis, the crack is a V-shaped notched of opening 2 mm as described in [9]. The solid 185 element is applied for meshing the 3D cracked beam in the ANSYS analysis. Figure 6 shows FEA results for the cracked cantilever beam mode shapes of bending vibration. Table 2 presents the results at different crack locations for crack depth 0.1 m obtained by 3D ANSYS analysis and

**Fig. 13** Sixth mode shape (third mode of bending vibration): cracked beam; ( $d/t = 0.55$ ,  $(e/L) = 0.1$ )



those obtained by Mia et al. [9] using 3D ABAQUS analysis. Plot of comparison results of frequency versus crack location from fixed end at the first three modes of bending vibration is presented in Fig. 7. The results in Table 2 and Fig. 7 showed that the variations can give validation for ANSYS FEA results, where the maximum variation is 1.86%.

**Modal Analysis**

The block Lanczos method was used to extract mode shapes and natural frequencies [23–26]. The natural frequencies of the first three modes of bending vibration for the intact cantilever beam model were validated by comparing the ANSYS FEA results to the values obtained using the analytical equation in Eq 5 [27]. The results of the two methods are listed in Table 3. The differences do not exceed – 2.4%.

$$\omega_n = (\beta_n l)^2 \sqrt{\frac{EI}{\rho A l^4}} \tag{Eq 5}$$

where  $\omega_n$  is the natural frequency describing the  $n$ -th mode of bending vibrations,  $E$  is Young’s modulus,  $I$  is the moment of inertia,  $\rho$  is the material density,  $A$  is the area of cross section, and  $l$  is the length of cantilever beam.

$$\beta_1 l = 1.875, \beta_2 l = 4.694, \text{ and for } n \geq 3 \beta_n l = (2n - 1)\pi/2$$

The first sixth natural frequencies of the intact and cracked cantilever beams are listed in Table 4. Figures 8, 9, 10, 11, 12, 13, 14 and 15 show mode shapes for the

cracked cantilever beam with a specified crack depth and crack location ratio. For the first three bending vibration mode shapes, the frequency ratio for the cracked beam was determined by calculating the ratio of the frequency of the cracked beam to that of the intact beam. The first three bending frequency ratios were plotted as a function of the crack depth ratio ( $d/t$ ) for varying crack location ratios ( $e/L$ ) in Figs. 16, 17 and 18. For the first mode of bending vibration, the frequency ratio decreased when the crack depth ratio increased and the crack location ratio decreased. For the second mode of bending vibration, the frequency ratio versus crack depth ratio at  $(e/L) = 0.5$  was less than that at  $(e/L) = 0.1$ , as shown in Fig. 17. This result was inconsistent because as the crack neared the fixed end of the beam, the frequency ratio should decrease. Further analysis showed that the Y-deformation that occurred at  $(e/L) = 0.5$  in the pattern of the second mode shape of bending vibration was greater than that at  $(e/L) = 0.1$ , as shown in Figs. 9 and 10. Also, the pattern of the third mode shape of bending vibration obtained using Fig. 18 where Y-deformation of this mode shape occurred at  $(e/L) = 0.5$  is slightly similar to that of the intact beam, as shown in Fig. 12. As a result, the frequency ratio versus crack depth ratio at  $(e/L) = 0.5$  is nearly equal to one. Y-deformation in the third mode of bending vibration occurred at  $(e/L) = 0.9$ , which is greater than that at  $(e/L) = 0.1$ , as shown in Figs. 11 and 13; this explains why the reason the frequency ratio for  $(e/L) = 0.9$  is less than that at  $(e/L) = 0.1$  in Fig. 18.

**Fig. 14** Sixth mode shape (first mode of torsional vibration): cracked beam; ( $d/t$ ) = 0.7, ( $e/L$ ) = 0.9

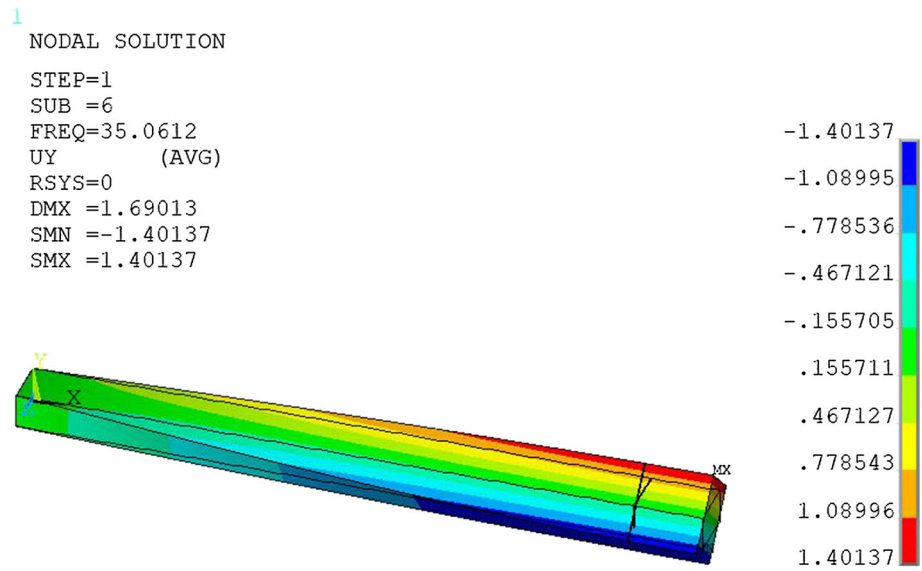


**Fig. 15** Fifth mode shape (first mode of torsional vibration): cracked beam; ( $d/t$ ) = 0.55, ( $e/L$ ) = 0.1

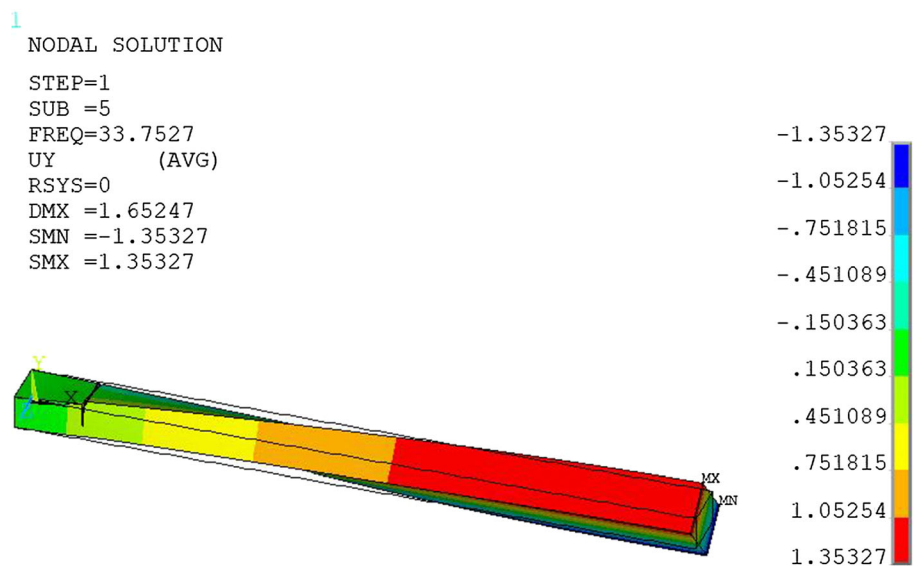


**Fig. 16** Frequency ratio vs. crack depth ratio at first mode of bending vibration

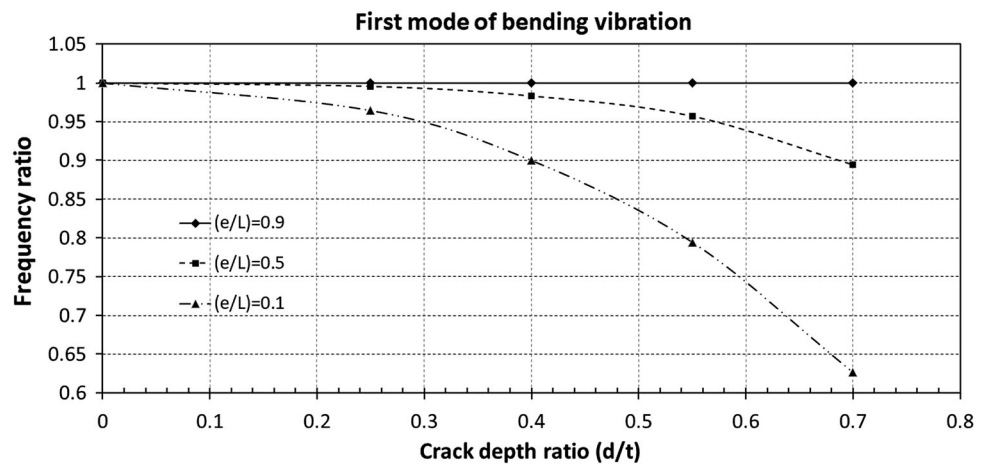


**Fig. 17** Frequency ratio vs. crack depth ratio at second mode of bending vibration

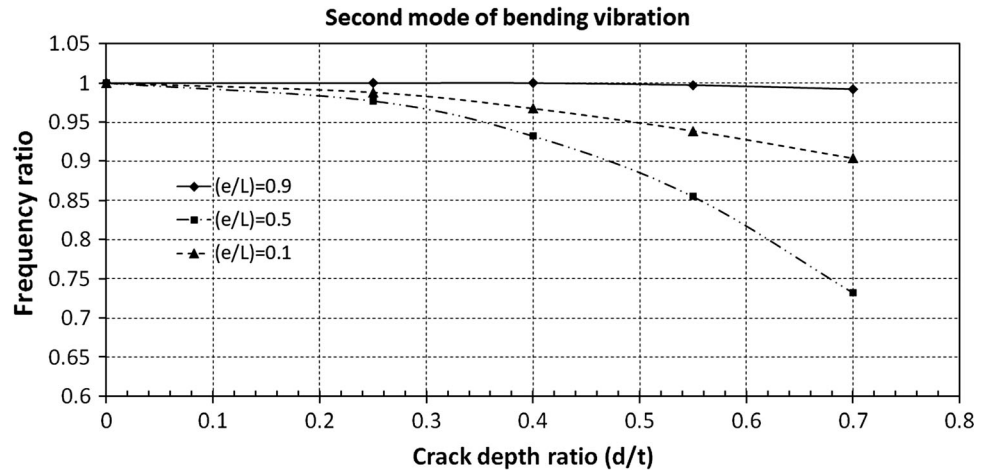


**Fig. 18** Frequency ratio vs. crack depth ratio at third mode of bending vibration

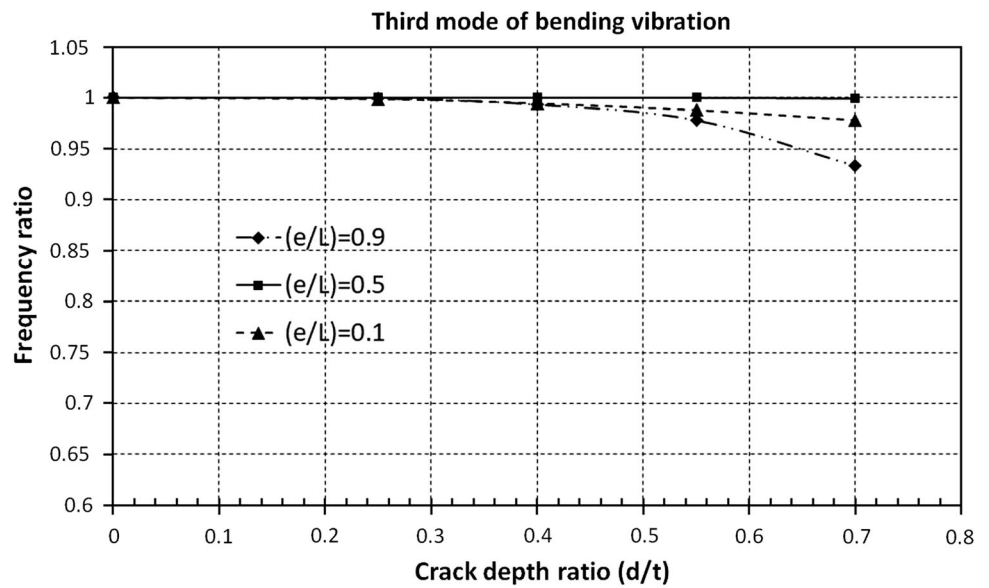


**Fig. 19** Zero frequency deflection: cracked beam; (d/t) = 0.7, (e/L) = 0.1

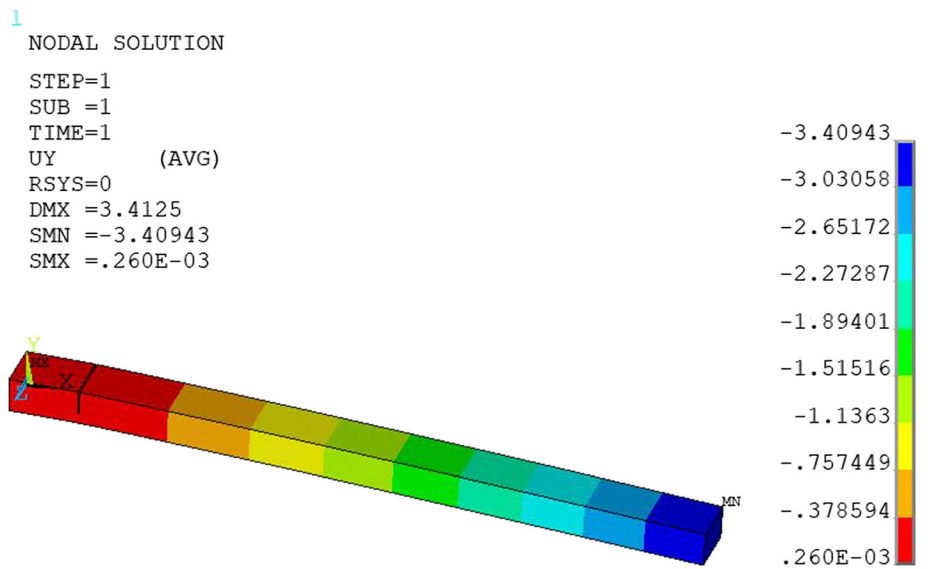


**Fig. 20** Zero frequency deflection: cracked beam; ( $d/t = 0.25$ ,  $e/L = 0.5$ )

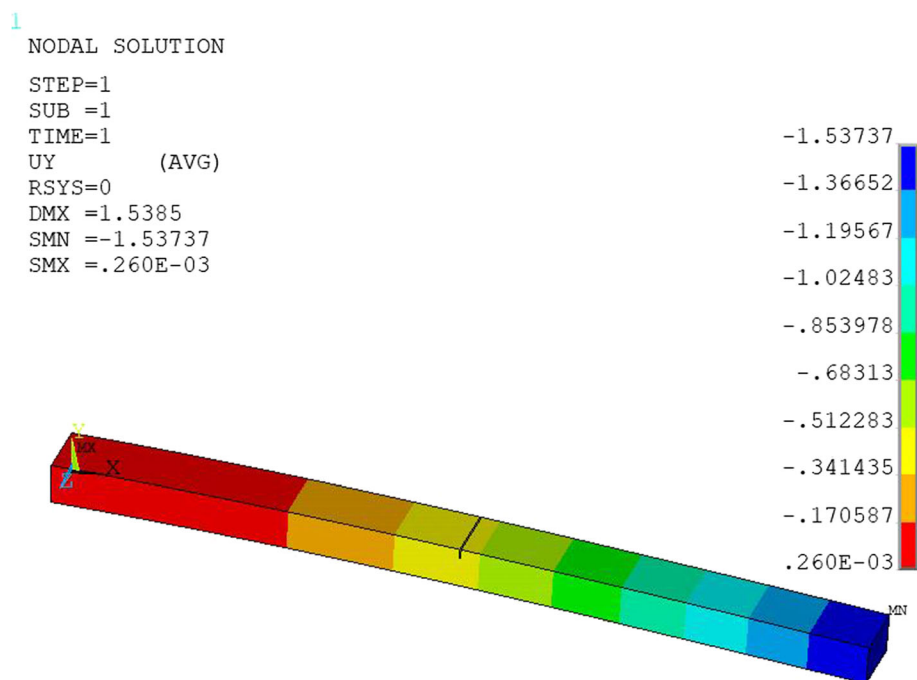
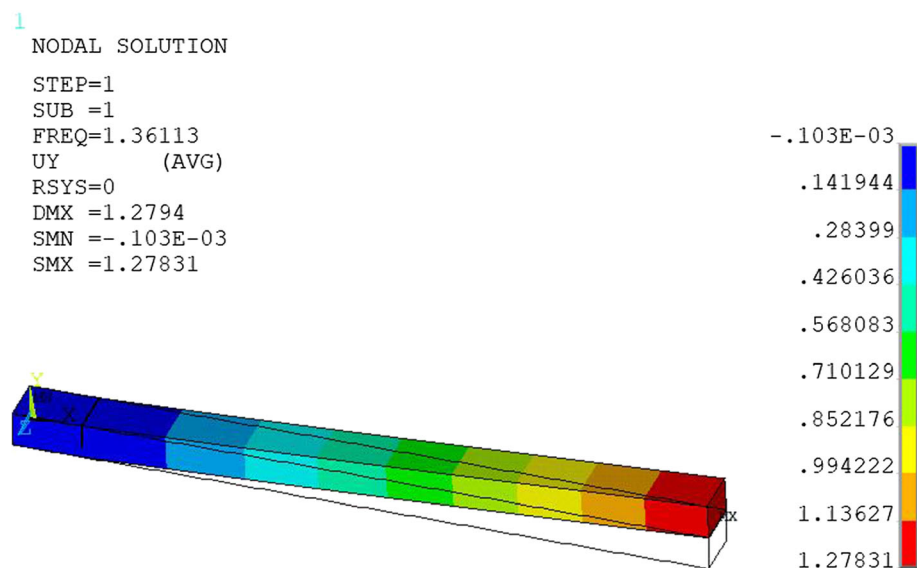


**Fig. 21** Natural frequency of the first mode of bending vibration: cracked beam; ( $d/t = 0.7$ ,  $e/L = 0.1$ )



### Stiffness of Intact and Cracked Cantilever Beam

Khalkar and Ramachandran [28] obtained the stiffness of the cracked beam by dividing the applied load at the free end of the cracked beam by the zero frequency deflection. The zero frequency deflection is obtained through a structural analysis of the deflection at the free end of the cantilever beam. The stiffness was validated using modal analysis to obtain the natural frequency of the first mode of bending vibration for the cracked beam and substituting it

in Eq 6 [28]. There was agreement in the computed stiffness calculated under the two methods. In this analysis, the stiffness of the intact and cracked beam was calculated using the same two methods indicated in [28]. The mass of the cracked cantilever beam was treated as identical to the mass of the intact cantilever beam, as the computed difference between these two masses was very small to negligible.

**Fig. 22** Natural frequency of the first mode of bending vibration: cracked beam; ( $d/t = 0.25$ ,  $e/L = 0.5$ )

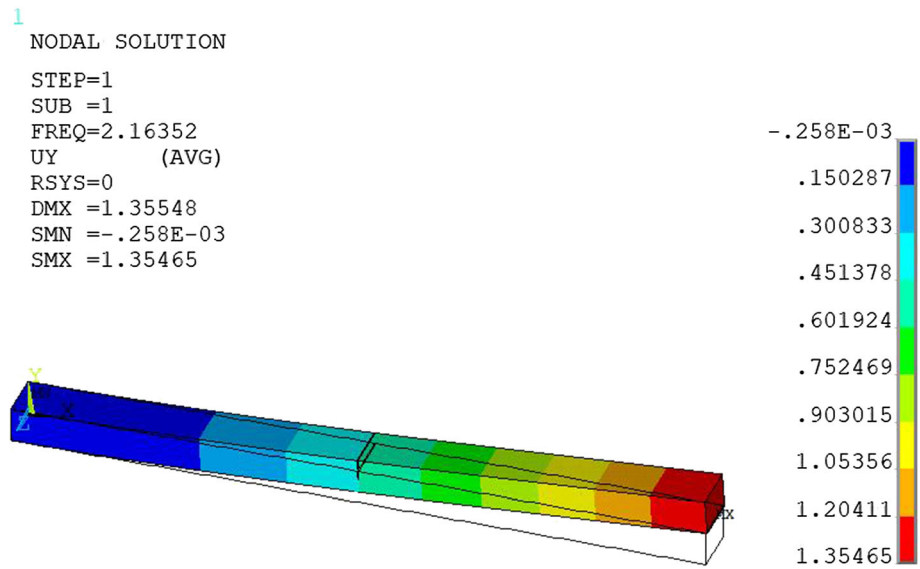


**Table 5** Stiffness of the intact and cracked cantilever beam

Object	Based on structural analysis		Based on modal analysis		
	Zero frequency deflection (mm)	Stiffness (N/mm)	Natural frequency of first mode of bending vibration (Hz)	Stiffness (N/mm)	Percent error (%)
Intact beam	1.51	99.3	2.1729	96.3	3.021
Cracked beam: ( $d/t = 0.25$ , $e/L = 0.1$ )	1.60	93.8	2.0956	89.6	4.478
Cracked beam: ( $d/t = 0.4$ , $e/L = 0.1$ )	1.8	83.3	1.9551	78	6.363
Cracked beam: ( $d/t = 0.55$ , $e/L = 0.1$ )	2.23	67.3	1.7263	60.8	9.658
Cracked beam: ( $d/t = 0.7$ , $e/L = 0.1$ )	3.41	44	1.3611	37.8	14.091
Cracked beam: ( $d/t = 0.25$ , $e/L = 0.5$ )	1.54	97.4	2.1635	95.5	1.951
Cracked beam: ( $d/t = 0.4$ , $e/L = 0.5$ )	1.6	93.8	2.1365	93.1	0.746
Cracked beam: ( $d/t = 0.55$ , $e/L = 0.5$ )	1.74	86.2	2.08	88.3	- 2.436
Cracked beam: ( $d/t = 0.7$ , $e/L = 0.5$ )	2.11	71.1	1.9432	77	- 8.298
Cracked beam: ( $d/t = 0.25$ , $e/L = 0.9$ )	1.51	99.3	2.1772	96.7	2.618
Cracked beam: ( $d/t = 0.4$ , $e/L = 0.9$ )	1.512	99.2	2.1779	96.8	2.419
Cracked beam: ( $d/t = 0.55$ , $e/L = 0.9$ )	1.52	98.7	2.1780	96.8	1.925
Cracked beam: ( $d/t = 0.7$ , $e/L = 0.9$ )	1.53	98	2.1786	96.8	1.224

$$f_n = \frac{1}{2\pi} \sqrt{\frac{k}{0.2357m}} \tag{Eq 6}$$

where  $k$  is the stiffness of an intact cantilever beam and 0.2357 m is the effective mass of an intact cantilever beam. Plots of the natural frequencies of the first mode of bending vibration and zero frequency deflection are shown in Figs. 19, 20, 21 and 22. The computed stiffness values for the intact and cracked cantilever beam are listed in Table 5.

### Harmonic Analysis

Harmonic analysis involves plotting the calculated response of a structure to cyclic loads over a frequency range on an amplitude versus frequency graph [23, 25]. Harmonic analysis is used to determine shifts in the natural frequencies and study the frequency response functions for the cracked beam [13]. The frequency response diagram is an important tool which can be used to detect a crack in the beam [2]. Ma et al. [29] analyzed the effects of excitation load and crack parameters on slant-cracked cantilever beam vibration responses. They used the amplitude

**Fig. 23** Deformation response in Y-direction for the cracked cantilever beam;  $(e/L) = 0.1$

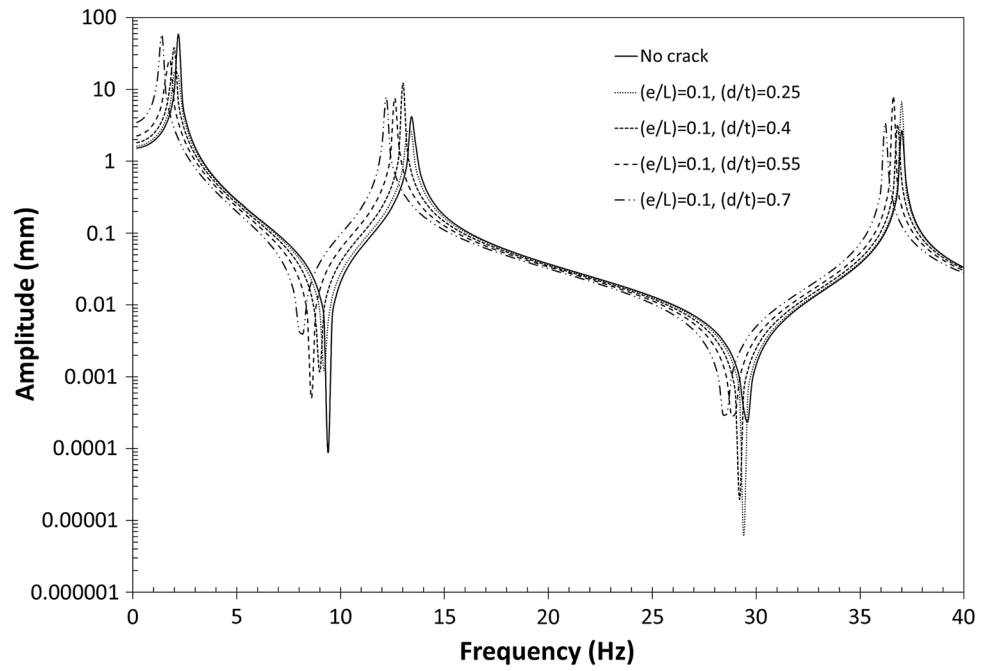


**Fig. 24** Deformation response in Y-direction for the cracked cantilever beam;  $(e/L) = 0.5$

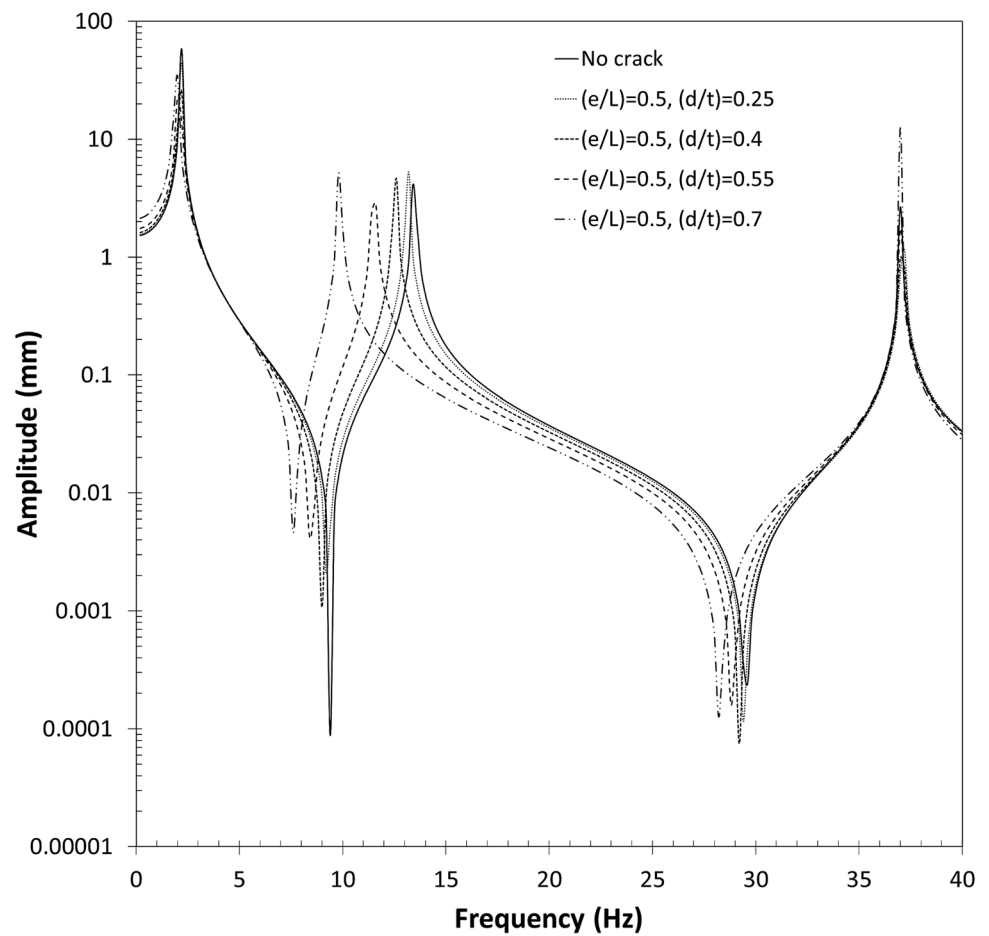


**Fig. 25** Deformation response in Y-direction for the cracked cantilever beam;  $(e/L) = 0.9$

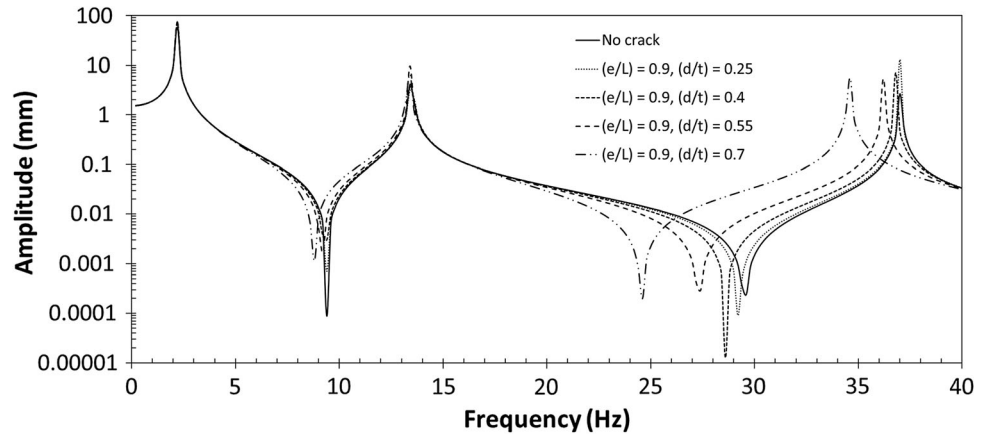
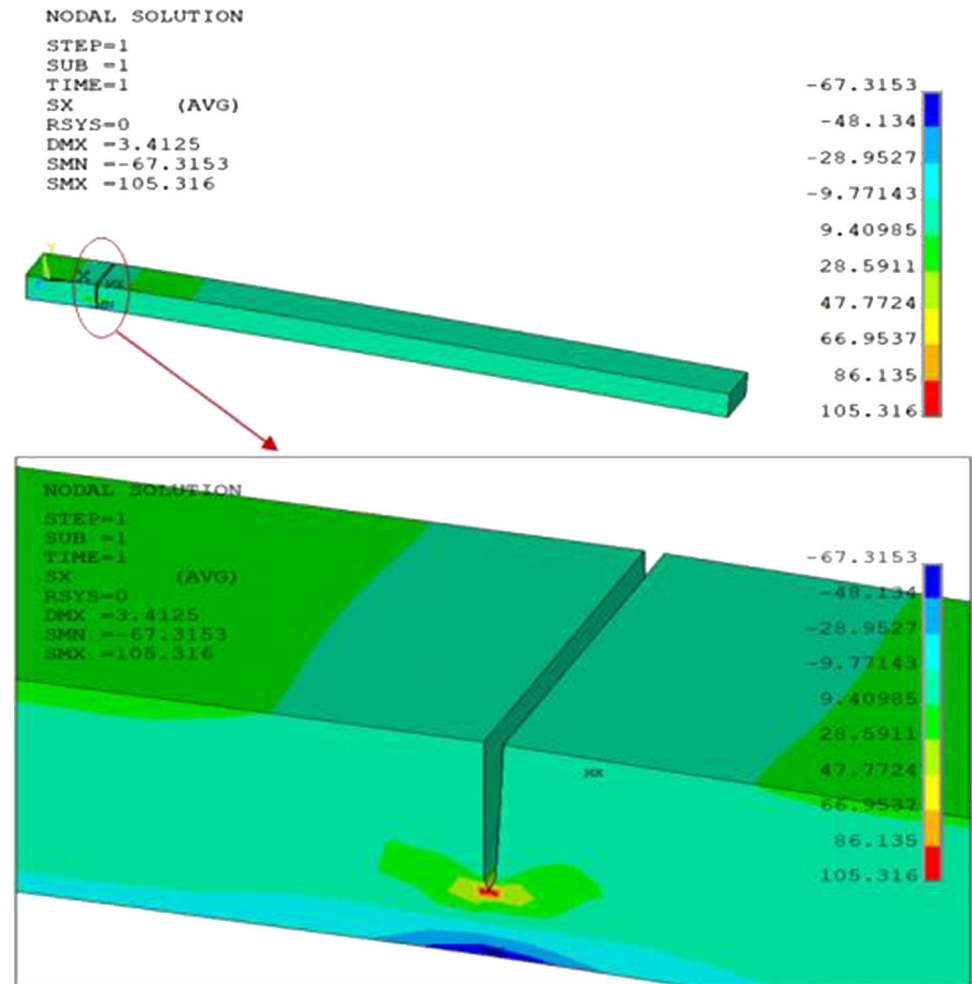


**Fig. 26** Enlarged view of the longitudinal stress distribution around the crack tip;  $(d/t) = 0.7$ ,  $(e/L) = 0.1$

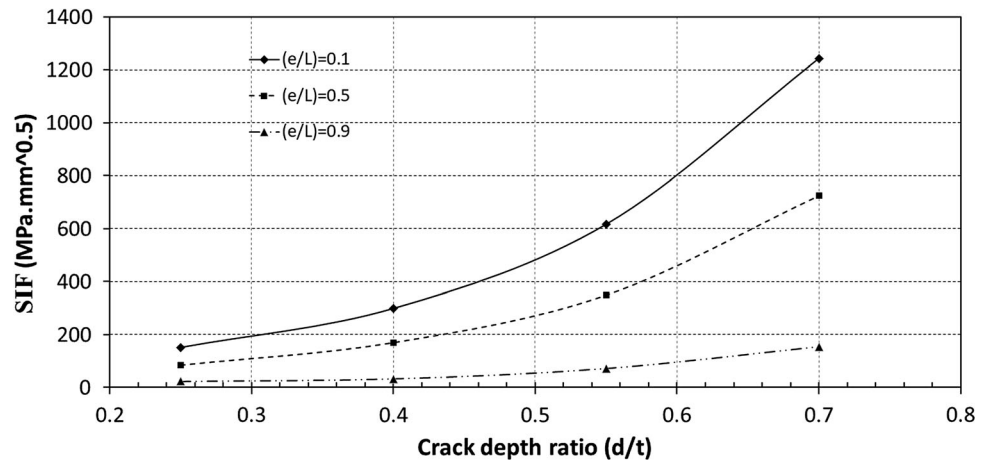


frequency responses in three frequency regions to describe the super-harmonic resonance, resonance and sub-harmonic resonance. In this study, harmonic analysis was used to examine the difference in the deformation responses in the Y-direction for the intact and cracked cantilever beams

at different crack depth ratios in specified crack locations. The deformation responses in the Y-direction in the range of 0–40 Hz are shown in Figs. 23, 24 and 25 for both the intact and cracked cantilever beams. The natural



**Fig. 27** Plot of SIF vs. crack depth ratio



frequencies of the cracked beam differ from those of the intact beam in the following ways:

1. For the first mode of bending vibration, (a) at  $(e/L) = 0.9$ , it is very small (at its lowest), (b) at  $(e/L) = 0.5$ , it increases, and (c) at  $(e/L) = 0.1$ , it increases more.
2. For the second mode of bending vibration, (a) at  $(e/L) = 0.9$ , it is very small (at its lowest), (b) at  $(e/L) = 0.1$ , it increases, and (c) at  $(e/L) = 0.5$ , it increases more (to its highest).
3. For the third mode of bending vibration, (a) at  $(e/L) = 0.5$ , it is very small (at its lowest), (b) at  $(e/L) = 0.1$ , it increases, and (c) at  $(e/L) = 0.9$ , it increases more (to its highest).

The observations in Figs. 23, 24 and 25 are used to establish the information in Figs. 16, 17 and 18 of the modal analysis and the pattern of mode shapes.

### Stress Intensity Factor

Stress intensity factor is defined as the crack driving force; its critical value is fracture toughness, a material property which reflects resistance to extension of the crack [30]. Stress intensity factor can be evaluated for three crack modes: mode I the crack is opening under tensile stress, mode II the crack is sliding under applied shear stress, and mode III the crack is tearing under applied shear stress [31]. The stress intensity factor denotes the severity of the crack. Many authors have presented studies on estimating the stress intensity factor for cracks [32–37].

The stress intensity factor for mode I (opening edge crack) was determined using Eq 7 [21]. ANSYS was used for a structural analysis of the stresses inside the crack. The contour of the longitudinal stress distribution around the crack tip for cracked cantilever beam  $(d/t) = 0.7$ ,  $(e/L) = 0.1$  is shown in Fig. 26. The SIF versus crack depth ratio was plotted for various crack locations in Fig. 27, showing that as crack depth ratio increased and crack location ratio decreased, the SIF values increased.

$L) = 0.1$  is shown in Fig. 26. The SIF versus crack depth ratio was plotted for various crack locations in Fig. 27, showing that as crack depth ratio increased and crack location ratio decreased, the SIF values increased.

$$SIF = \sigma \sqrt{\pi d} f(d/t) \quad (\text{Eq 7})$$

$$f(d/t) = 1.13 - 1.374(d/t) + 5.749(d/t)^2 - 4.464(d/t)^3$$

where SIF is the first stress intensity factor,  $\sigma$  is stress in the crack,  $d$  is crack depth, and  $t$  is the thickness of the cantilever beam.

### Conclusions

Based on the results obtained in this study, the following conclusions were drawn:

1. An increase in crack depth led to decreased rotational stiffness and increased flexibility in the crack.
2. At specific crack locations, the reduction in the natural frequencies of the cracked cantilever beam was proportional to the depth of crack.
3. For the first bending vibration mode, the natural frequency of the cracked cantilever beam was proportional to the distance of the crack from the fixed end of the cantilever beam.
4. For the second and third bending vibration modes, the pattern of mode shapes was vital to understanding the variation in the natural frequency of the cracked cantilever beam.
5. In the modal analysis, plotting the deformation responses in the Y-direction for the intact and cracked cantilever beams revealed a noticeable shift in the natural frequencies.
6. Where the depth of the crack was constant, the stiffness of the cracked beam increased as the distance

of the crack from the fixed end of the cantilever beam increased.

7. Where the location of the crack was constant, the stiffness of the cracked beam decreased as the crack depth increased.
8. Stress intensity factor values in mode I increased as crack depth increased and the distance of the crack from the fixed end of the cantilever beam decreased.

## References

1. M. Behzad, A. Meghdari, A. Ebrahimi, A new approach for vibration analysis of a cracked beam. *Int. J. Eng. Trans. B Appl.* **18**(4), 319–330 (2005)
2. M. Heydari, A. Ebrahimi, M. Behzad, Forced vibration analysis of a Timoshenko cracked beam using a continuous model for the crack. *Eng. Sci. Technol. Int. J.* **17**(4), 194–204 (2014)
3. S. Choudhury, D.N. Thatoi, K. Maity, S. Sau, M.D. Rao, A modified support vector regression approach for failure analysis in beam-like structures. *J. Fail. Anal. Prev.* **18**(4), 998–1009 (2018)
4. D.K. Agarwalla, D.R. Parhi, Effect of crack on modal parameters of a cantilever beam subjected to vibration, in *Chemical, Civil and Mechanical Engineering Tracks of 3rd Nirma University International Conference on Engineering*. (Ahmedabad, India, 2012), Procedia Engineering, 2013, vol. 51, pp. 665–669
5. A. Banerjee, G. Pohit, Crack investigation of rotating cantilever beam by fractal dimension analysis, in *2nd International Conference on Innovations in Automation and Mechatronics Engineering*. (Vallabh Vidyanagar, India, 2014), Procedia Technology, 2014, vol. 14, pp. 188–195
6. I.A. Khan, D.R. Parhi, Finite element analysis of double cracked beam and its experimental validation, in *Chemical, Civil and Mechanical Engineering Tracks of 3rd Nirma University International Conference on Engineering*. (Ahmedabad, India, 2012), Procedia Engineering, 2013, vol. 51, pp. 703–708
7. J. Liu, W.D. Zhu et al., A dynamic model of a cantilever beam with a closed, embedded horizontal crack including local flexibilities at crack tips. *J. Sound Vib.* **382**, 274–290 (2016)
8. J. Zeng, H. Ma, W. Zhang, B. Wen, Dynamic characteristic analysis of cracked cantilever beams under different crack types. *Eng. Fail. Anal.* **74**, 80–94 (2017)
9. M.S. Mia, M.S. Islam, U. Ghosh, Modal analysis of cracked cantilever beam by finite element simulation, in *10th International Conference on Marine Technology*. (Dhaka, Bangladesh, 2016), Procedia Engineering, 2017, vol. 194, pp. 509–516
10. B.P. Nandwana, S.K. Maiti, Modelling of vibration of beam in presence of inclined edge or internal crack for its possible detection based on frequency measurements. *Eng. Fract. Mech.* **58**(3), 193–205 (1997)
11. V.R. Khalkar, S. Ramachandran, Study of free undamped and damped vibrations of a cracked cantilever beam. *J. Eng. Sci. Technol.* **13**(2), 449–462 (2018)
12. A.K. Batabyal, P. Sankar, T.K. Paul, Crack detection in cantilever beam using vibration response. ed by E. Inan et al. *Vibration Problems ICOVP-2007*. Springer Proc. Phys. vol. 126, pp. 27–33 (2008)
13. M. Djidrov, V. Gavriloski, J. Jovanova, Vibration analysis of cantilever beam for damage detection. *FME Trans.* **42**, 311–316 (2014)
14. R.K. Behera, A. Pandey, D.R. Parhi, Numerical and experimental verification of a method for prognosis of inclined edge crack in cantilever beam based on synthesis of mode shapes, in *2nd International Conference on Innovations in Automation and Mechatronics Engineering*. (Vallabh Vidyanagar, India, 2014), Procedia Technology, 2014, vol. 14, pp. 67–74
15. A. Ciciello, A. Palmeri, Static analysis of Euler–Bernoulli beams with multiple unilateral cracks under combined axial and transverse loads. *Int. J. Solids Struct.* **51**(5), 1020–1029 (2014)
16. M.J. Mungla, D.S. Sharma, R.R. Trivedi, Identification of a crack in clamped-clamped beam using frequency-based method and genetic algorithm, in *12th International Conference on Vibration Problems, ICOVP*. (Guwahati, India, 2015), Procedia Engineering, 2016, vol. 144, pp. 1426–1434
17. A.D. Dimarogonas, S.A. Paipetis, *Analytical Methods in Rotor Dynamics* (Elsevier, London, 1983)
18. P.F. Rigos, N. Aspragathos, A.D. Dimarogonas, Identification of crack location and magnitude in a cantilever beam from the vibration modes. *J. Sound Vib.* **138**(3), 381–388 (1990)
19. K.H. Barad, D.S. Sharma, V. Vyas, Crack detection in cantilever beam by frequency based method, in *Chemical, Civil and Mechanical Engineering Tracks of 3rd Nirma University International Conference on Engineering*. (Ahmedabad, India, 2012), Procedia Engineering, 2013, vol. 51, pp. 770–775
20. A.J. Dentsoras, A.D. Dimarogonas, Resonance controlled fatigue crack propagation in a beam under longitudinal vibrations. *Int. J. Fract.* **23**(1), 15–22 (1983)
21. W.M. Ostachowicz, M. Krawczuk, Analysis of the effect of cracks on the natural frequencies of a cantilever beam. *J. Sound Vib.* **150**(2), 191–201 (1991)
22. Y. Nakasone, S. Yoshimoto, T.A. Stolarski, *Engineering Analysis Using ANSYS Software* (Elsevier Butterworth-Heinemann, Oxford, 2006)
23. M.A.B. Marzuki, M.H.A. Halim, A.R.N. Mohamed, Determination of natural frequencies through modal and harmonic analysis of space frame race car chassis based on ANSYS. *Am. J. Eng. Appl. Sci.* **8**(4), 538–548 (2015)
24. V. Khalkar, S. Ramachandran, Free vibration study of v-shape and rectangular shape double-sided cracks in a cantilever beam. *J. VibroEng.* **19**(2), 1026–1038 (2017)
25. E.S.M.M. Soliman, Static and vibration analysis of CFRP composite mono leaf spring. *J. Fail. Anal. Prev.* **19**(1), 5–14 (2019)
26. M.V.M.O. Filho et al., Analysis of sensor placement in beams for crack identification. *Lat. Am. J. Solids Struct.* **15**(11), 1–18 (2018)
27. M. Romaszko, B. Sapinski, A. Sioma, Forced vibrations analysis of a cantilever beam using the vision method. *J. Theor. Appl. Mech.* **53**(1), 243–254 (2015)
28. V. Khalkar, S. Ramachandran, The effect of crack geometry on stiffness of spring steel cantilever beam. *J. Low Freq. Noise Vib. Act. Control.* **0**, 1–13 (2018)
29. H. Ma, J. Zeng et al., Analysis of the dynamic characteristics of a slant-cracked cantilever beam. *Mech. Syst. Signal Process.* **75**, 261–279 (2016)
30. N. Perez, *Fracture Mechanics* (Kluwer Academic Publishers, Boston, 2004)
31. R. Shao, F. Dong et al., Influence of cracks on dynamic characteristics and stress intensity factor of gears. *Eng. Fail. Anal.* **32**, 63–80 (2013)
32. R.G. Ahangar, Y. Verreman, Assessment of mode I and mode II stress intensity factors obtained by displacement extrapolation and interaction integral methods. *J. Fail. Anal. Prev.* **19**(1), 85–97 (2019)
33. Y. Liao, Y. Li et al., Residual fatigue life analysis of cracked aluminum lithium alloy plates repaired with titanium alloy patches for different sizes. *J. Fail. Anal. Prev.* **19**(1), 258–269 (2019)

34. V. Sivakumar, K.P. Dani, S. Sriram, Prediction of stress intensity factor on precracked composite wing rib made up of carbon-epoxy IM7-8552. *J. Fail. Anal. Prev.* **16**(4), 635–646 (2016)
35. A.Y.T. Leung, Z. Zhou, X. Xu, Determination of stress intensity factors by the finite element discretized symplectic method. *Int. J. Solids Struct.* **51**(5), 1115–1122 (2014)
36. S.J. Rouzegar, M. Mirzaei, Modeling dynamic fracture in Kirchhoff plates and shells using the extended finite element method. *Sci. Iran.* **20**(1), 120–130 (2013)
37. J. Wang, X.Q. Zhang et al., Investigation of fatigue growth behavior of an inclined crack in aluminum alloy plate. *J. Fail. Anal. Prev.* **18**(5), 1159–1167 (2018)

**Publisher's Note** Springer Nature remains neutral with regard to jurisdictional claims in published maps and institutional affiliations.